AEM
Journals.ASM.org

Alcohol Selectivity in a Synthetic Thermophilic *n*-Butanol Pathway Is Driven by Biocatalytic and Thermostability Characteristics of Constituent Enzymes

Andrew J. Loder,[a] Benjamin M. Zeldes,[a] G. Dale Garrison II,[a] Gina L. Lipscomb,[b] Michael W. W. Adams,[b] Robert M. Kelly[a]

Department of Chemical and Biomolecular Engineering, North Carolina State University, Raleigh, North Carolina, USA[a]; Department of Biochemistry and Molecular Biology, University of Georgia, Athens, Georgia, USA[b]

***n*-Butanol is generated as a natural product of metabolism by several microorganisms, but almost all grow at mesophilic temperatures. A synthetic pathway for *n*-butanol production from acetyl coenzyme A (acetyl-CoA) that functioned at 70°C was assembled *in vitro* from enzymes recruited from thermophilic bacteria to inform efforts for engineering butanol production into thermophilic hosts. Recombinant versions of eight thermophilic enzymes (β-ketothiolase [Thl], 3-hydroxybutyryl-CoA dehydrogenase [Hbd], and 3-hydroxybutyryl-CoA dehydratase [Crt] from *Caldanaerobacter subterraneus* subsp. *tengcongensis*; *trans*-2-enoyl-CoA reductase [Ter] from *Spirochaeta thermophila*; bifunctional acetaldehyde dehydrogenase/alcohol dehydrogenase [AdhE] from *Clostridium thermocellum*; and AdhE, aldehyde dehydrogenase [Bad], and butanol dehydrogenase [Bdh] from *Thermoanaerobacter* sp. strain X514) were utilized to examine three possible pathways for *n*-butanol. These pathways differed in the two steps required to convert butyryl-CoA to *n*-butanol: Thl-Hbd-Crt-Ter-AdhE (*C. thermocellum*), Thl-Hbd-Crt-Ter-AdhE (*Thermoanaerobacter* X514), and Thl-Hbd-Crt-Ter-Bad-Bdh. *n*-Butanol was produced at 70°C, but with different amounts of ethanol as a coproduct, because of the broad substrate specificities of AdhE, Bad, and Bdh. A reaction kinetics model, validated via comparison to *in vitro* experiments, was used to determine relative enzyme ratios needed to maximize *n*-butanol production. By using large relative amounts of Thl and Hbd and small amounts of Bad and Bdh, >70% conversion to *n*-butanol was observed *in vitro*, but with a 60% decrease in the predicted pathway flux. With more-selective hypothetical versions of Bad and Bdh, >70% conversion to *n*-butanol is predicted, with a 19% increase in pathway flux. Thus, more-selective thermophilic versions of Bad, Bdh, and AdhE are needed to fully exploit biocatalytic *n*-butanol production at elevated temperatures.**

Metabolic engineering for biomass-based fuel or chemical production has focused almost exclusively on mesophilic host organisms, although now thermophilic hosts are also being considered, as molecular genetic tools become available (1–4). Thermal bioprocesses can be advantageous for a variety of reasons (5). Extreme thermophiles (optimum temperature [T_{opt}] of ≥70°C), in particular, could be especially strategic for industrial processes, due to lower risk of contamination, facilitated product recovery, and reduced cooling costs, factors which must be weighed against energy requirements to maintain bioprocesses at elevated temperatures (6, 7).

In principle, thermophilic metabolic engineering platforms can potentially draw from an enzyme inventory encompassing a broad temperature range (8–10). However, one must take into account potential issues with synthetic pathways comprised of heterologous enzymes with variable levels of thermoactivity and thermostability. This factor can be exacerbated by the relative scarcity of biochemically and biophysically characterized versions of specific thermophilic enzymes of interest. As such, biocatalysts may need to be recruited from sources with functional temperature ranges that are inconsistent with the thermophilic host, leading to incompatibility between the activity and stability among enzymes selected for use in an engineered pathway. For example, metabolic engineering of *Caldicellulosiruptor bescii* (T_{opt} = 78°C) for increased ethanol production utilized an enzyme from *Clostridium thermocellum* (T_{opt} = 60°C), resulting in product formation only at 65°C or below (11). An additional challenge for metabolic engineering at any temperature is balancing biocatalytic function among pathway enzymes. High-level expression of all heterologous genes in a pathway can lead to poor product titers and yields, underscoring the need for tuning gene expression to improve overall performance (12, 13). This strategy is often actuated through trial and error or combinatorial approaches, although more-deterministic computational methods have been proposed (14, 15). Similarly, achieving commercially viable titers and yields in thermophilic hosts will require strain optimization, which becomes challenging as the functional properties of constituent pathway enzymes become more disparate.

Biological butanol production has received significant attention lately, driven by concerns about energy sustainability and anthropogenic global climate change (16–18). *n*-Butanol has long been utilized as a solvent and feedstock for chemical production processes, but it can additionally be used as a drop-in gasoline

Received 1 July 2015 **Accepted** 29 July 2015

Accepted manuscript posted online 7 August 2015

Citation Loder AJ, Zeldes BM, Garrison GD, II, Lipscomb GL, Adams MWW, Kelly RM. 2015. Alcohol selectivity in a synthetic thermophilic *n*-butanol pathway is driven by biocatalytic and thermostability characteristics of constituent enzymes. Appl Environ Microbiol 81:7187–7200. doi:10.1128/AEM.02028-15.

Editor: A. M. Spormann

Address correspondence to Robert M. Kelly, rmkelly@ncsu.edu.

Supplemental material for this article may be found at http://dx.doi.org/10.1128/AEM.02028-15.

doi:10.1128/AEM.02028-15

replacement due to its superior fuel properties; *n*-butanol has an energy density and octane number similar to those of gasoline (19–21). Thermophilic production of volatile products, such as fuel alcohols, allows for the possibility of facilitated product removal. The use of thermophilic organisms would be a favorable match for most separation processes recovering butanol from dilute fermentation broth, including distillation, gas stripping, and pervaporation (22). For example, for a solution of *n*-butanol (20 g/liter) in water, the relative volatility increases from 5.6 at 30°C to 16 at 70°C, as predicted by the UNIQUAC model (AspenPlus, v8.0; Aspen Technology, Inc., Bedford, MA). Thus, gas stripping to concentrate *n*-butanol from a dilute solution in a fermentor would be greatly facilitated by using a thermophilic host.

n-Butanol is produced natively by multiple fermentative bacteria in the genus *Clostridium*; in fact, *Clostridium acetobutylicum* fermentation was the primary method of butanol production until petroleum-based processes became more cost-effective (19). In native producers, *n*-butanol is made from acetyl coenzyme A (acetyl-CoA), using electrons donated from NADH via a five-enzyme pathway composed of a β-ketothiolase (Thl; EC 2.3.1.16), 3-hydroxybutyryl-CoA dehydrogenase (Hbd; EC 1.1.1.35), 3-hydroxybutyryl-CoA dehydratase (Crt; EC 4.2.1.55), butyryl-CoA dehydrogenase (Bcd/Etf), and a bifunctional acetaldehyde dehydrogenase/alcohol dehydrogenase (AdhE; EC 1.2.1.10 and 1.1.1.1) (Fig. 1) (19, 23, 24). All of the enzymes are NADH dependent, with the exception of Bcd/Etf, which catalyzes an electron-bifurcating reaction to transfer electrons from two molecules of NADH to oxidized ferredoxin (Fd_{ox}) and crotonyl-CoA (2 NADH + Fd_{ox} + crotonyl-CoA → 2 NAD^+ + Fd_{red}^{2-} + butyryl-CoA) (23). Using this native pathway, along with other modifications, clostridia have been metabolically engineered for increased butanol production, with titers reported up to 19 g/liter (Table 1) (25–27).

n-Butanol production has also been engineered into a diverse set of more genetically tractable mesophiles, with the highest batch titer reported in *Escherichia coli* at 15 g/liter (Table 1). The pathway was adapted for *E. coli* by replacing Bcd/Etf with a *trans*-2-enoyl-CoA reductase (Ter; EC 1.3.1.44) to balance ferredoxin metabolism (24). Ter directly uses NADH to reduce crotonyl-CoA, alleviating the need to recycle reduced ferredoxin produced by Bcd/Etf, while making the reaction irreversible and thus providing a "kinetic trap" in the pathway (28, 29).

All organisms producing significant amounts (>0.1 g/liter) of *n*-butanol, engineered or not, also produce large quantities of ethanol. In cases where the *C. acetobutylicum* enzymes are used for the aldehyde/alcohol dehydrogenase activity (e.g., *E. coli*, *C. acetobutylicum*, and *Thermoanaerobacterium saccharolyticum*), more *n*-butanol is produced relative to ethanol than when native aldehyde/alcohol dehydrogenase enzymes are used (e.g., *Lactobacillus brevis* and *Saccharomyces cerevisiae*). This effect is likely due to the increased selectivity of *C. acetobutylicum* AdhE, Bad, and Bdh for four-carbon substrates (30, 31). Additionally, increased production of reducing equivalents or knocking out genes encoding enzymes that produce more oxidized fermentation products, both of which change the host's redox balance, can increase *n*-butanol production (1, 24, 32). Thus, the ratio of ethanol to *n*-butanol production seems to depend upon the specificity of the aldehyde dehydrogenase (Bad or AdhE) and alcohol dehydrogenase (Bdh or AdhE) for four-carbon substrates, although redox balancing of substrates and fermentation products also plays a role.

Reports of butanol production in thermophiles are sparse. The

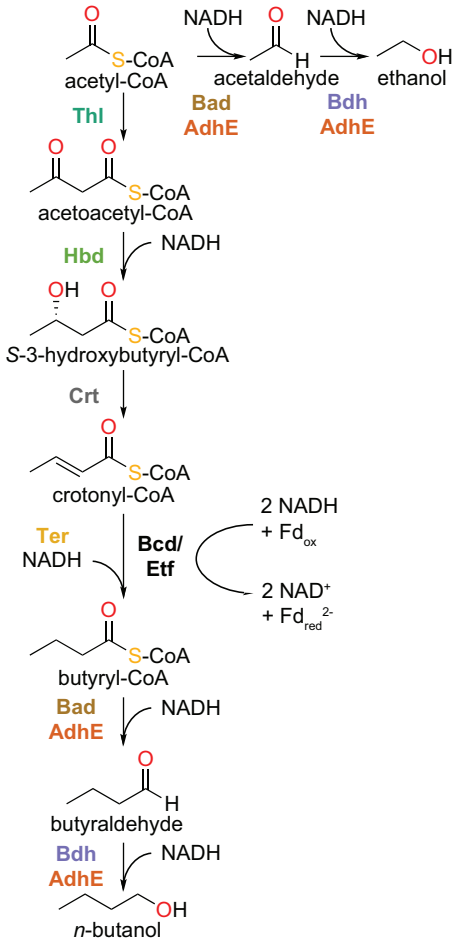

FIG 1 Enzymatic pathway for *n*-butanol formation. Abbreviations: Thl, β-ketothiolase (EC 2.3.1.16); Hbd, 3-hydroxybutyryl-CoA dehydrogenase (EC 1.1.1.35); Crt, 3-hydroxybutyryl-CoA dehydratase (EC 4.2.1.55); Bcd/Etf, butyryl-CoA dehydrogenase/electron transfer protein; Ter, *trans*-2-enoyl-CoA reductase (EC 1.3.1.44); Bad, aldehyde dehydrogenase (EC 1.2.1.10); Bdh, alcohol dehydrogenase (EC 1.1.1.1); AdhE, bifunctional acetaldehyde dehydrogenase/alcohol dehydrogenase; Fd_{ox}, oxidized ferredoxin; Fd_{red}, reduced ferredoxin.

highest temperature for native *n*-butanol production is 58°C in *Clostridium thermosaccharolyticum* (33), although trace amounts are produced by *Pyrodictium abyssi* (T_{opt} = 110°C) (34). In engineered organisms, *n*-butanol has been produced by *Thermoanaerobacterium thermosaccharolyticum* and *T. saccharolyticum* at 55°C (Table 1). To date, there is only one report of *n*-butanol being produced by an extreme thermophile growing above 60°C. *Pyrococcus furiosus*, a hyperthermophile (T_{opt} = 100°C), was metabolically engineered to produce alcohols via a hybrid pathway assembled *in vivo*, based on thermophilic versions of enzymes related to those found in *C. acetobutylicum* (35). Production of ethanol and *n*-butanol resulted in low titers, yields, and selectivities at 60°C, due in part to the fact that enzymes from microbial sources with T_{opt} values of 60 to 75°C were utilized (35). In this work, we use a reaction kinetics model, informed by *in vitro*-measured enzyme biochemical and biophysical (i.e., thermostability) properties, to explore possible routes to improving *n*-butanol–ethanol selectivity in engineered strains of *P. furiosus* or other

TABLE 1 *n*-Butanol production by selected native and engineered microorganisms

Microorganism	Temp (°C)	Butanol titer (g/liter)	Ethanol titer (g/liter)[a]	Reference
Clostridium acetobutylicum (native)	37	17	0.92	26
Clostridium thermosaccharolyticum (native)	58	1.9	5.1	33
Clostridium acetobutylicum (engineered)	37	19	2	27
Escherichia coli	37	15	2	24
Thermoanaerobacterium thermosaccharolyticum	55	0.38	0.86	67
Thermoanaerobacterium saccharolyticum	55	0.85	1.8	1
Lactobacillus brevis	30	0.30	4.6	68
Saccharomyces cerevisiae	30	0.25[b]	4–8	69
		0.0025	NR	70
Pseudomonas putida	30	0.12	NR	71
Synechococcus elongatus	30	0.030	NR	72
Bacillus subtilis	37	0.024	NR	71

[a] NR, not reported.
[b] Using a modified leucine synthesis pathway instead of the clostridial pathway.

thermophilic hosts. The model provided key insights into how enzyme characteristics, relative enzyme concentrations, and enzyme stability impact selectivity for *n*-butanol production relative to the less-desired product ethanol. It also defines the desired kinetic properties for specific enzymes in a hybrid thermophilic pathway to maximize *n*-butanol formation.

MATERIALS AND METHODS

Materials. Strains and vectors used for cloning included competent *E. coli* NovaBlue cells and competent *E. coli* Rosetta 2(DE3) cells (EMD Millipore, Billerica, MA) and pET-28b, pET-21b, and pET-46 Ek/LIC cloning kit. The primers were purchased from IDT (Coralville, IA). Reagents and devices used include the following: acetyl-CoA, acetoacetyl-CoA, (*S*)-3-hydroxybutyryl-CoA, crotonyl-CoA, butyryl-CoA, butyraldehyde, acetaldehyde, NADH, 1 mg/ml bovine serum albumin protein standard, and protein molecular mass standards (Sigma-Aldrich, St. Louis, MO); buffer components, medium components, and GelCode blue stain reagent (Thermo Fisher Scientific, Pittsburgh, PA); NuPAGE 4 to 12% Bis-Tris protein gels and BenchMark protein standards (10 to 220 kDa) (Life Technologies, Grand Island, NY); Bio-Rad protein assay dye reagent (Hercules, CA); QIAquick PCR purification and QIAprep spin miniprep kits (Qiagen, Inc., Valencia, CA); restriction enzymes, Gibson assembly master mix, and Quickload DNA ladder (1 kb) (New England BioLabs, Ipswich, MA); Amicon Ultra 10K centrifugal filter units (EMD Millipore, Billerica, MA); HisTrap HP, HiLoad Q-Sepharose XK 16/10, HiLoad Superdex 200 pg 26/600, and Superdex 200 10/300 GL fast-performance liquid chromatography (FPLC) columns (GE Healthcare); ZB-WAXplus capillary gas chromatography (GC) column (30 m long, 0.53-mm inner diameter [ID], 1-μm film thickness) (Phenomenex, Torrance, CA).

Recombinant production of pathway enzymes. TTE0544 (*crt*), TTE0548 (*hbd*), TTE0549 (*thl*), Teth514_1935 (X514-*bdh*), and Teth514_1942 (X514-*bad*) were amplified by PCR from genomic DNA (gDNA) (*Caldanaerobacter subterraneus* subsp. *tengcongensis* DSM 15242 or *Thermoanaerobacter* sp. strain X514 ATCC BAA-938) using primers shown in Table S1 in the supplemental material and ligated into pET-46 Ek/LIC. Cthe_0423 (*C. thermocellum adhE* [*Ctherm-adhE*]) was amplified by PCR from *C. thermocellum* ATCC 27405 genomic DNA and ligated into pET-21b between the NdeI and XhoI restriction sites. Teth514_0627 (*Thermoanaerobacter* sp. strain X514 *adhE* [X514-*adhE*]) was amplified from gDNA by PCR and ligated into pET-28b between the NcoI and XhoI restriction sites using Gibson assembly (36). Stherm_c16300 (*ter*) was codon optimized for *E. coli* and synthesized (Life Technologies) and then ligated into pET-28b between the NcoI and NotI restriction sites. Competent *E. coli* NovaBlue GigaSingles cells were transformed with ligation products and plated on LB agar medium containing appropriate antibiotics. Colonies were cultured in liquid LB medium with appropriate antibiotics, and extracted plasmids were sequenced by Eton Bioscience, Inc. (Durham, NC) or Genewiz, Inc. (Research Triangle Park, NC).

Competent *E. coli* Rosetta 2(DE3) cells were transformed with expression vectors and plated on LB agar with appropriate antibiotics. Single colonies were cultured overnight in ZYM-5052 autoinduction medium (37) at 37°C with 275 rpm rotary shaking. Expression cultures were harvested by centrifugation at 6,000 × *g* for 10 min, resuspended in lysis buffer (300 mM NaCl, 50 mM sodium phosphate, 1 mM $MgCl_2$, 20 mM imidazole, 10% glycerol [pH 8.0]), and lysed with a French press pressure cell at 16,000 lb/in^2. Lysis buffer for *Ctherm*-AdhE and X514-AdhE also contained 3 mM dithiothreitol (DTT), and 0.5 mM phenylmethanesulfonyl fluoride. Crude homogenate was incubated at 60°C for 30 min to precipitate most *E. coli* proteins and then centrifuged at 25,000 × *g* for 20 min to obtain cell extracts.

All recombinant enzymes were first purified by immobilized metal affinity chromatography at room temperature using 1-ml HisTrap HP columns. Buffers had the same composition as lysis buffer, and protein was eluted with a linear gradient of 20 to 500 mM imidazole. Active fractions were pooled, concentrated, and exchanged into 25 mM Tris-HCl, 1 mM $MgCl_2$, and 3 mM DTT (pH 8.0) using 10,000 (10K) centrifugal filters, mixed with an equal volume of glycerol, and stored at −20°C.

Crt was further purified by anion-exchange chromatography at room temperature on a HiLoad Q-Sepharose XK16/10 column in 25 mM Tris-HCl, 1 mM $MgCl_2$, and 10% glycerol (pH 8.0) and eluted with a linear gradient of 0 to 1 M NaCl. Fractions from peaks with activity were pooled, concentrated, and stored as described above.

Ctherm-AdhE and X514-AdhE were further purified by gel filtration chromatography at 4°C on a HiLoad Superdex 200 pg 26/600 column in 50 mM sodium phosphate, 150 mM NaCl, 1 mM $MgCl_2$, 3 mM DTT, and 10% (vol/vol) glycerol (pH 7.8). Active fractions were pooled, concentrated, and stored as described above.

Enzyme activity assays. All enzyme assays monitored consumption of NADH spectrophotometrically at 340 nm, using an extinction coefficient of 6,300 M^{-1} cm^{-1} (38). All assay reactions were performed in 120-μl volumes in quartz cuvettes with 1-cm path length. The enzyme was preheated with 100 mM morpholinepropanesulfonic acid (MOPS)-KOH (pH 7.9 at 22°C) and 0.3 mM NADH, and the reaction was started by the addition of substrate. Assays of the two AdhE enzymes were carried out at 60°C, and all other assays were conducted at 70°C. Thl and Crt do not oxidize NADH, so coupled assays with Hbd and Ter were used, respectively, where at least 10-fold excess of the coupled enzymes ensured that Thl and Crt would be rate determining. Michaelis-Menten kinetic parameters and standard errors were determined using the R package (R Foundation for Statistical Computing) with nlstools (39).

A range of at least six different substrate concentrations was used for each enzyme. Thl was assayed on 50 to 5,000 μM acetyl-CoA and a final enzyme concentration of 1.4 μg/ml, with the coupled Hbd enzyme at 66.7 μg/ml. Hbd was assayed on 3 to 500 μM acetoacetyl-CoA and 0.4 μg/ml enzyme. Crt was assayed on 25 to 5,000 μM 3-hydroxybutyryl-CoA and 0.3 μg/ml enzyme, with the coupled Ter enzyme at 186 μg/ml. Ter was assayed on 10 to 1,000 μM crotonyl-CoA and 2.2 μg/ml enzyme. *Thermoanaerobacter* sp. strain X514 Bad (X514-Bad) was assayed on 10 to 500 μM acetyl-CoA or 5 to 500 μM butyryl-CoA, with 5.3 μg/ml enzyme. X514-Bdh was assayed on 0.25 to 20 mM acetaldehyde or 0.1 to 20 mM butyraldehyde with 3.1 μg/ml enzyme. X514-AdhE was assayed on 5 to 500 μM acetyl-CoA, 5 to 500 μM butyryl-CoA, 0.625 to 20 mM acetaldehyde, or 0.625 to 20 mM butyraldehyde, with 16.25 μg/ml enzyme. *Ctherm*-AdhE was assayed on 10 to 500 μM acetyl-CoA, 10 to 500 μM butyryl-CoA, 0.5 to 40 mM acetaldehyde, or 0.625 to 40 mM butyraldehyde, with 20 μg/ml enzyme.

To determine enzyme thermostability, enzyme was incubated in 100 mM MOPS-KOH (pH 7.9 at 22°C) and 0.3 mM NADH at 60°C or 70°C for times ranging from 1 min to 19 h. Following the incubation, residual enzyme activity was assayed at 70°C. Enzyme activity over time was fit to a two-step enzyme inactivation mechanism (40):

$$E \xrightarrow{k_1} E_1\ (\beta) \xrightarrow{k_2} E_d$$

where E is the fully active enzyme, E_1 is an intermediate with lower activity β, E_d is inactive enzyme, and k_1 and k_2 are rate constants. The fractional activity y at time t is modeled by

$$y(t) = [1 + \beta k_1/(k_2 - k_1)]\ \exp(-k_1 t) - \beta k_1/(k_2 - k_1)\ \exp(-k_2 t) \quad (1)$$

In the case where there is no active intermediate (E_1), the equation reduces to first-order decay:

$$y(t) = \exp(-k_1 t) \quad (2)$$

Enzyme inactivation data were fit to equation 1 unless β or k_1 were indeterminate, in which case equation 2 was used.

***In vitro n*-butanol production.** For *in vitro* conversion of acetyl-CoA to *n*-butanol, the reaction mixture contained MOPS-KOH buffer (100 mM, pH 7.9 at 22°C), acetyl-CoA (5 mM), NADH (40 mM), and enzymes (various concentrations). The reaction mixtures were incubated at 60°C or 70°C for 45 min and then cooled on ice. The internal standard 2-butanol was added to a final concentration of 250 μg/ml, and the mixtures were analyzed for alcohol production by gas chromatography. All reactions were run in triplicate.

Gas chromatography. Alcohols were quantified with a Shimadzu GC-2014 gas chromatograph equipped with a ZB-WAXplus capillary column (30 m long, 0.53-mm ID, 1-μm film thickness) and flame ionization detector. The GC oven temperature was initially held at 40°C for 2 min, increased to 240°C at 20°C/min, and held for 9 min. The injector and detector temperatures were held at 310°C and 250°C, respectively. Nitrogen was used as the carrier gas at a column flow of 30 cm/s. Sample volumes of 0.5 μl were injected with a 1:10 split ratio using an AOC-20i autosampler.

Kinetic modeling and optimization. The concentrations of pathway intermediates over time were modeled by constructing a system of differential mass balance equations based on known reaction stoichiometry, rate law expressions, and enzyme parameters reported below (see Tables 4 and 5). Any unknown parameters were estimated using literature on homologous enzymes. Reactions with calculated equilibrium constants greater than 100 ($\Delta G^{\circ\prime} < -11.4$ kJ/mol at pH 7.0) were modeled as irreversible; all other reactions were modeled as reversible. The differential equations were solved using the ode15s function in MATLAB (version R2011b; Mathworks, Inc.) for given initial compound concentration enzyme concentrations. Enzyme inactivation was modeled by adjusting the enzyme concentrations over time according to equation 1.

To predict optimized enzyme ratios, the model was used to construct a nonlinear optimization problem to minimize an objective function, which was the final ratio of ethanol to butanol after the reaction had proceeded to completion. The objective function was minimized by changing the enzyme concentrations subject to two constraints. First, the total enzyme mass was fixed. Second, the minimum allowed concentration of any enzyme was set to 10% of the concentration used for the base case, where the base case used enzyme concentrations such that each enzyme was present at the same activity of 0.2 U/ml. For each case, the minimization problem was solved 50 times using randomized enzyme concentrations to avoid local minima.

Other methods. Protein concentrations were determined by the method of Bradford using Bio-Rad protein assay dye reagent with bovine serum albumin as the standard (41). SDS-PAGE was done using NuPAGE 4 to 12% Bis-Tris polyacrylamide gels with MOPS buffer and stained with GelCode blue. Enzyme molecular masses were determined by size exclusion chromatography with a Superdex 200 10/300 GL column, using buffer containing 50 mM sodium phosphate, 150 mM NaCl, 1 mM $MgCl_2$, 1 mM DTT, and 10% (vol/vol) glycerol (pH 7.8) at 0.5 ml/min.

RESULTS

Selection of thermophilic enzymes for hybrid pathway. Because no extreme thermophile contains all of the enzymes necessary for *n*-butanol production from acetyl-CoA, genes encoding such enzymes from multiple sources are obviously required. Additionally, few of the required enzymes from extreme thermophiles have been characterized. Therefore, a homology search strategy was used to select potential extremely thermophilic candidates for each type of enzyme (Table 2), as reported previously (35). Three variations of the pathway can be constructed from these enzymes, which vary only in the identity of the enzyme(s) used to catalyze the last two pathway steps: *Ctherm*-AdhE, X514-AdhE, or Bad and Bdh (Fig. 1). All three pathway variations use Ter, rather than the NADH- and ferredoxin-dependent bifurcating Bcd/Etf system that is found in native *n*-butanol producers. Use of the Bcd/Etf system as part of the pathway *in vivo* would produce reduced ferredoxin, which would then have to be reoxidized by the host, leading to a potential imbalance in ferredoxin metabolism; substituting Ter for the Bcd/Etf system avoids this ferredoxin imbalance.

Production of enzymes from hybrid pathway. Each enzyme was heterologously expressed in *E. coli* and isolated to a purity of ~80% or greater, as determined by SDS-PAGE image densitometry (Fig. 2 and Table 2). *Ctherm*-AdhE and X514-AdhE purified by immobilized metal affinity chromatography (IMAC) contained low-molecular-mass contaminants, most of which were removed by size exclusion chromatography. These low-molecular-mass bands were also observed in IMAC-purified AdhE after expression under anaerobic conditions or at reduced temperature (18°C or 30°C). Anion-exchange chromatography likewise could not remove these bands, indicating that the polypeptides comprising these bands have pIs that are very similar to the pI of the full-length AdhE. Thus, these low-molecular-mass bands are likely the result of AdhE degradation by *E. coli* and do not represent native *E. coli* proteins, since heat treatment and IMAC alone were able to purify most of the other enzymes to homogeneity. Although *Ctherm*-AdhE activity has been characterized in cell extracts (42, 43), purified forms of *Ctherm*-AdhE and X514-AdhE have not been previously characterized.

Kinetic parameters for enzymes in the hybrid *n*-butanol pathway. The kinetic parameters (V_{max} and K_m) of each purified enzyme were determined *in vitro*, using NADH as the reductant,

TABLE 2 Hybrid thermophilic *n*-butanol pathway enzymes

Source thermophilic microorganism	Growth T_{opt} (°C)	Enzyme	Query gene[a]	Thermophile locus tag	Homology to query (Cov-ID-Pos)[e]	Monomer MM[b] (kDa)		Purity[c] (%)	Enzyme MM[d] (kDa)	Molecular assembly
						Sequence-predicted	SDS-PAGE			
Caldanaerobacter subterraneus subsp. *tengcongensis*	75	Thl	CA_C2873	TTE0549	99-68-83	43.6	42.3	98	158	α_4
	75	Hbd	CA_C2708	TTE0548	99-70-84	32.8	34.4	86	206	α_6
	75	Crt	CA_C2712	TTE0544	98-60-80	30.0	29.7	79	92	α_3
Spirochaeta thermophila	68	Ter	TDE_0597	STHERM_c16300	98-56-73	45.4	47.1	83	43	α_1
Clostridium thermocellum	60	AdhE	CA_P0035	Cthe_0423	99-64-82	97.2	94.3	81	254	α_3
Thermoanaerobacter sp. strain X514	60	AdhE	CA_P0035	Teth514_0627	99-53-72	97.7	94.9	79	535	α_6
	60	Bad	Cbei_3832	Teth514_1942	92-50-68	51.7	52.4	88	265	α_5
	60	Bdh	CA_C3298	Teth514_1935	99-29-49	44.0	40.4	82	79	α_2

[a] CA, *Clostridium acetobutylicum*; TDE, *Treponema denticola*; Cbei, *Clostridum beijerinckii*.
[b] MM, molecular mass.
[c] Determined by SDS-PAGE image densitometry.
[d] Determined by gel filtration chromatography.
[e] Cov-ID-Pos, percent coverage, percent identity, and percent positives.

to facilitate insight into operation of the assembled pathway (Table 3 and Fig. 3). The kinetics of all enzymes were determined at 70°C with the exception of the two AdhE enzymes, which were assayed at 60°C due to the observed decrease in *Ctherm*-AdhE activity after less than 1 min when assayed at 70°C. The three alcohol dehydrogenases examined here, X514-Bdh, *Ctherm*-AdhE, and X514-AdhE, were assayed by their aldehyde reduction activity. All have low V_{max} and high apparent K_m values on both acetaldehyde and butyraldehyde (Fig. 3A). These enzymes have k_{cat}/K_m values ranging from 2.4×10^3 to 7.1×10^3 M^{-1} s^{-1} for butyraldehyde, 2- to 7-fold higher than that for acetaldehyde, making them only slightly specific for butyraldehyde. The NADH-dependent Bdh from *C. acetobutylicum* has k_{cat}/K_m values of 304 and 6.1 M^{-1} s^{-1} on butyraldehyde and acetaldehyde, respectively, making it highly specific for butyraldehyde (44). Similarly, NADPH-dependent Bdh from *Clostridium beijerinckii* has high specificity, with a k_{cat}/K_m 100-fold higher for butyraldehyde than for acetaldehyde (45). X514-Bdh, *Ctherm*-AdhE, and X514-AdhE, as well as *C. acetobutylicum* Bdh, all have K_m values for aldehydes above 2 mM, well above the intracellular butyraldehyde concentration measured in *C. acetobutylicum*, which was less than 1 mM (46). Thus, rates of ethanol or *n*-butanol production in *Thermoanaerobacter* sp. strain X514, *C. thermocellum*, and *C. acetobutylicum* are in the linear portion of the Michaelis-Menten curve and, therefore, sensitive to acetaldehyde or butyraldehyde concentration. This may help draw the pathway toward alcohol production due to the near-irreversibility of the reaction, although much of the maximum aldehyde reductase activity would be underutilized (44). An additional issue is that none of the alcohol dehydrogenases examined here have any strong preference for butyraldehyde over acetaldehyde, which is important for maintaining pathway selectivity for production of *n*-butanol relative to ethanol.

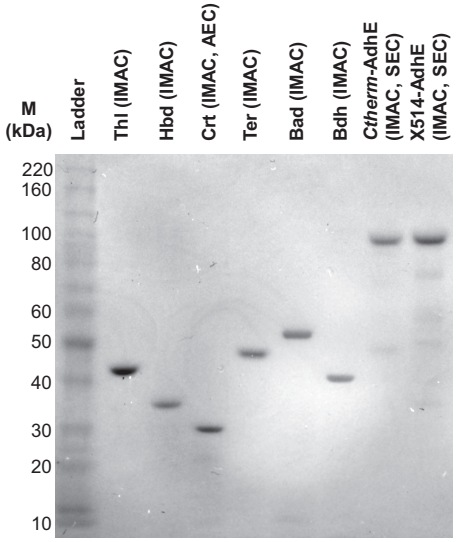

FIG 2 SDS-PAGE analysis of purified enzymes. The positions of molecular mass markers (M) (in kilodaltons) are shown to the left of the gel. Abbreviations: IMAC, immobilized metal affinity chromatography; AEC, anion-exchange chromatography; SEC, size exclusion chromatography.

Similarly, the three aldehyde dehydrogenases, X514-Bad, *Ctherm*-AdhE, and X514-AdhE, which were assayed by their acyl-CoA reduction activity, are not highly specific for either acetyl-CoA or butyryl-CoA (Fig. 3B). Neither AdhE examined here showed significant preference for butyryl-CoA over acetyl-CoA as a substrate, with nearly identical k_{cat}/K_m values for both substrates. However, X514-Bad shows some substrate specificity, with k_{cat}/K_m for butyryl-CoA 15-fold higher than that for acetyl-CoA. This is similar to the Bad found in *C. beijerinckii*, which has a k_{cat}/K_m 7-fold higher for butyryl-CoA than for acetyl-CoA (47). These results suggest that using X514-Bad would allow greater selectivity for production of *n*-butanol relative to ethanol than either of the two AdhE enzymes.

The V_{max} of the recombinant, His-tagged *Ctherm*-AdhE reported here has an activity of 2.2 ± 0.3 U/mg for acetaldehyde reduction (Table 3), much lower than expected considering that the reported activity of AdhE in *C. thermocellum* cell extract is 7.7 ± 0.1 U/mg using a similar assay (42). Reported acetaldehyde reductase activities of purified AdhE from a variety of organisms vary widely. Recombinant versions of AdhE from *C. acetobutylicum* and *Thermoanaerobacter ethanolicus* have activities of 0.18 and 2.6 U/mg, respectively, similar to or much less than the value obtained here for *Ctherm*-AdhE (48, 49). In contrast, native puri-

TABLE 3 Kinetic parameters of *n*-butanol pathway enzymes[a]

Enzyme	Locus tag	Substrate	*Km* (μM)	V_{max} (U/mg)[b]	k_{cat}/K_m (10^3 M^{-1} s^{-1})
Thl	TTE0549	Acetyl-CoA	271 ± 48	74.2 ± 3.1	199 ± 36
Hbd	TTE0548	Acetoacetyl-CoA	18.7 ± 3.4	64.1 ± 2.9	1,880 ± 350
Crt	TTE0544	3-Hydroxybutyryl-CoA	107 ± 19	533 ± 18	2,490 ± 430
Ter	Stherm_c16300	Crotonyl-CoA	49.9 ± 14.1	63.1 ± 3.9	956 ± 276
Ctherm-AdhE	Cthe_0423	Acetyl-CoA	11.5 ± 1.0	2.01 ± 0.04	283 ± 26
		Butyryl-CoA	15.0 ± 3.1	1.41 ± 0.07	152 ± 32
		Acetaldehyde	7,760 ± 2,240	2.21 ± 0.26	0.46 ± 0.15
		Butyraldehyde	6,920 ± 870	9.53 ± 0.48	2.27 ± 0.30
X514-AdhE	Teth514_0627	Acetyl-CoA	9.40 ± 1.16	2.20 ± 0.06	381 ± 48
		Butyryl-CoA	5.71 ± 0.66	1.38 ± 0.03	394 ± 46
		Acetaldehyde	22,000 ± 4,800	14.1 ± 1.6	1.09 ± 0.30
		Butyraldehyde	3,230 ± 20	14.0 ± 0.3	7.11 ± 0.49
X514-Bad	Teth514_1942	Acetyl-CoA	83.6 ± 31.6	5.31 ± 0.64	55.3 ± 21.7
		Butyryl-CoA	27.2 ± 6.3	26.4 ± 1.6	833 ± 198
X514-Bdh	Teth514_1935	Acetaldehyde	3,330 ± 850	10.6 ± 0.9	2.37 ± 0.59
		Butyraldehyde	2,030 ± 340	14.1 ± 0.7	5.13 ± 0.89

[a] Uncertainties represent one standard error.
[b] 1 U = 1 μmol of product formed/min. All V_{max} values were determined using 0.3 mM NADH as a cofactor.

fied AdhE from *E. coli*, *Geobacillus thermoglucosidasius*, and *Entamoeba histolytica* have higher acetaldehyde reductase activities of 9.9, 51, and 320 U/mg, respectively, although the *E. coli* activity is only ~5-fold greater than the *Ctherm*-AdhE activity (50–52). The native forms of AdhE are known to form large multimeric structures called spirosomes containing 20 or more AdhE monomers (50–52). The spirosomes are hypothesized to enhance catalytic efficiency through substrate channeling of acetaldehyde or by sta-

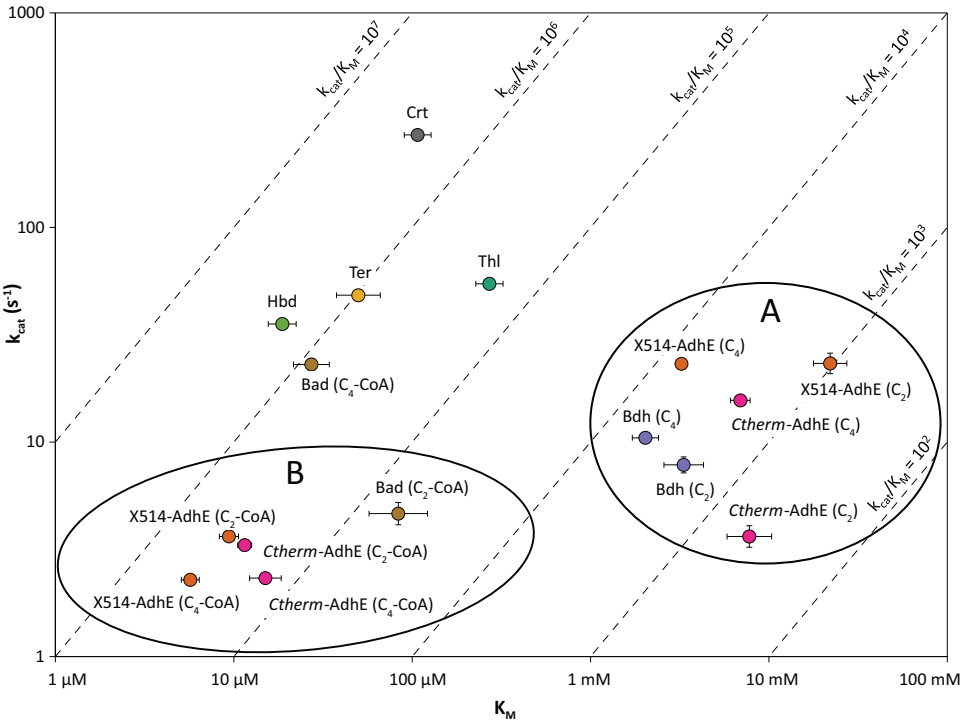

FIG 3 Kinetic parameters of *n*-butanol pathway enzymes in log space. The broken lines represent constant values of k_{cat}/K_m. Substrate abbreviations: C_2, acetaldehyde; C_4, butyraldehyde; C_2-CoA, acetyl-CoA; C_4-CoA, butyryl-CoA. Each error bar represents one standard error.

TABLE 4 Inactivation parameters of *n*-butanol pathway enzymes[a]

Enzyme	Inactivation parameter[b]							
	70°C				60°C			
	β	k_1 (10^{-3} min^{-1})	k_2 (10^{-3} min^{-1})	$t_{1/2}$ (min)	β	k_1 (10^{-3} min^{-1})	k_2 (10^{-3} min^{-1})	$t_{1/2}$ (min)
Thl		3.36 ± 0.65		206		2.12 ± 0.34		327
Hbd		0.20 ± 0.08		3,470		0.10 ± 0.09		6,930
Crt		4.17 ± 1.06		166		0.10 ± 0.12		6,930
Ter		4.59 ± 0.48		151		0.32 ± 0.08		2,170
Bad[c]	0.70 ± 0.06	315 ± 174	6.88 ± 1.71	52.1	0.43 ± 0.04	204 ± 38	5.49 ± 2.55	9.49
Bdh[d]	0.13 ± 0.01	385 ± 21	60.5 ± 3.2	2.18	0.58 ± 0.03	370 ± 65	10.6 ± 1.4	16.9
Ctherm-AdhE[d]		1169 ± 178		0.59		2.52 ± 0.06		275
X514-AdhE[d]	0.68 ± 0.05	622 ± 225	32.8 ± 3.7	11.0		1.03 ± 0.08		673

[a] Enzyme inactivation data were fit to a two-step enzyme inactivation model or a simple first-order inactivation model. The two-step enzyme inactivation mechanism or one-step inactivation model were calculated by using the following equations:

$$y(t) = [1 + \beta k_1/(k_2 - k_1)]\ \exp(-k_1 t) - \beta k_1/(k_2 - k_1)\ \exp(-k_2 t)$$

and

$$y(t) = \exp(-k_1 t)$$

[b] Uncertainties represent one standard error. $t_{1/2}$, half-life.
[c] With butyryl-CoA as the substrate.
[d] With butyraldehyde as the substrate.

bilizing the protein (51), which may explain some of the discrepancy between activities reported for native and recombinant forms. Clearly, the native form of *Ctherm*-AdhE should be studied further to resolve the discrepancy between activities of the recombinant version and native cell extract.

Enzyme stability. Because of the importance of enzyme stability in thermophilic metabolic engineering applications, the stability of each enzyme at pH 7.9 and 60°C or 70°C was determined. Enzyme inactivation data were fit to a two-step enzyme inactivation model or a simple first-order inactivation model if it provided an adequate fit (Table 4). Thl, Hbd, Crt, and Ter inactivate slowly at 70°C, with half-lives longer than 2 h, and are extremely stable at 60°C with half-lives greater than 6 h, consistent with the fact that they come from organisms with T_{opt} values of ≥70°C. Because X514-Bad, X514-Bdh, and both AdhE enzymes are from microorganisms with T_{opt} values of 60°C, it was not surprising that they inactivated quickly at 70°C. *Ctherm*-AdhE was particularly unstable at 70°C with a half-life of <1 min, although it is quite stable at 60°C with a half-life of 275 min. The Bad enzyme quickly decreases to 70% residual activity at 70°C and 43% activity at 60°C, but then it is inactivated much more slowly. The Bdh enzyme behaves similarly to Bad at 60°C, but it loses most of its activity within a few minutes at 70°C. These results indicate that *Ctherm*-AdhE is not stable enough for use in a host growing near 70°C.

***In vitro* assembly of *n*-butanol pathway.** To confirm that the purified enzymes can be used together to produce *n*-butanol, they were assembled *in vitro*. Two variations of the pathway were examined, differing only in the enzymes used to convert butyryl-CoA to *n*-butanol: Thl-Hbd-Crt-Ter-Bad-Bdh, and Thl-Hbd-Crt-Ter-AdhE (*Thermoanaerobacter* strain X514). The pathway variant using *Ctherm*-AdhE was not examined because of its poor stability at 70°C, making it unsuitable for use in an extremely thermophilic host, such as *P. furiosus*, growing at 70°C or above. Enzymes for the Bad/Bdh and X514-AdhE pathways were mixed in equal proportions based on specific activity, corresponding to the molar enzyme proportions seen in Fig. 4A. These enzyme mixtures were incubated at 60°C and 70°C with a high acetyl-CoA concentration (5 mM) and a stoichiometric excess of NADH (40 mM) to allow complete conversion of acetyl-CoA and accurate quantification of the resulting alcohols by gas chromatography. The theoretical maximum conversion of acetyl-CoA to alcohols (100%) was achieved by both pathways (Fig. 4B and C). However, the enzyme mixtures had a low selectivity for *n*-butanol production, with the Bad/Bdh and X514-AdhE pathways converting 28% and 5% of carbon to *n*-butanol, respectively, with the balance being ethanol.

Pathway kinetic modeling and optimization. To gain further insight into the operation of the complete pathway, a kinetic model was implemented using measured enzyme parameters and appropriate rate law expressions (Tables 5 and 6). The model predicts species concentrations over time for given initial substrate and enzyme concentrations. While kinetic models have been used to examine a variety of metabolic pathways, including the acetone-butanol-ethanol (ABE) pathway in *C. acetobutylicum*, most kinetic models have required fitting parameters to data from batch fermentation experiments (53, 54). In contrast, our model used *a priori*-determined kinetic parameters for individual enzymes; no parameters were adjusted to fit measured *n*-butanol or ethanol production by the assembled pathways.

The primary goal for using the kinetic model was to identify ways to increase the selectivity of *n*-butanol production versus ethanol production. The final concentrations achieved in the modeled reaction can be used to determine the selectivity, defined as the molar ratio of carbon in *n*-butanol to carbon in ethanol. One strategy for increasing the selectivity is to change the enzyme ratios, which is analogous to changing the relative expression levels of enzymes *in vivo*. Optimum enzyme ratios for *n*-butanol selectivity could be determined by searching the enzyme concentration space to minimize the final ethanol concentration. The optimization search was subject to a fixed total enzyme mass, an approximation of the cellular energy investment in the pathway enzymes.

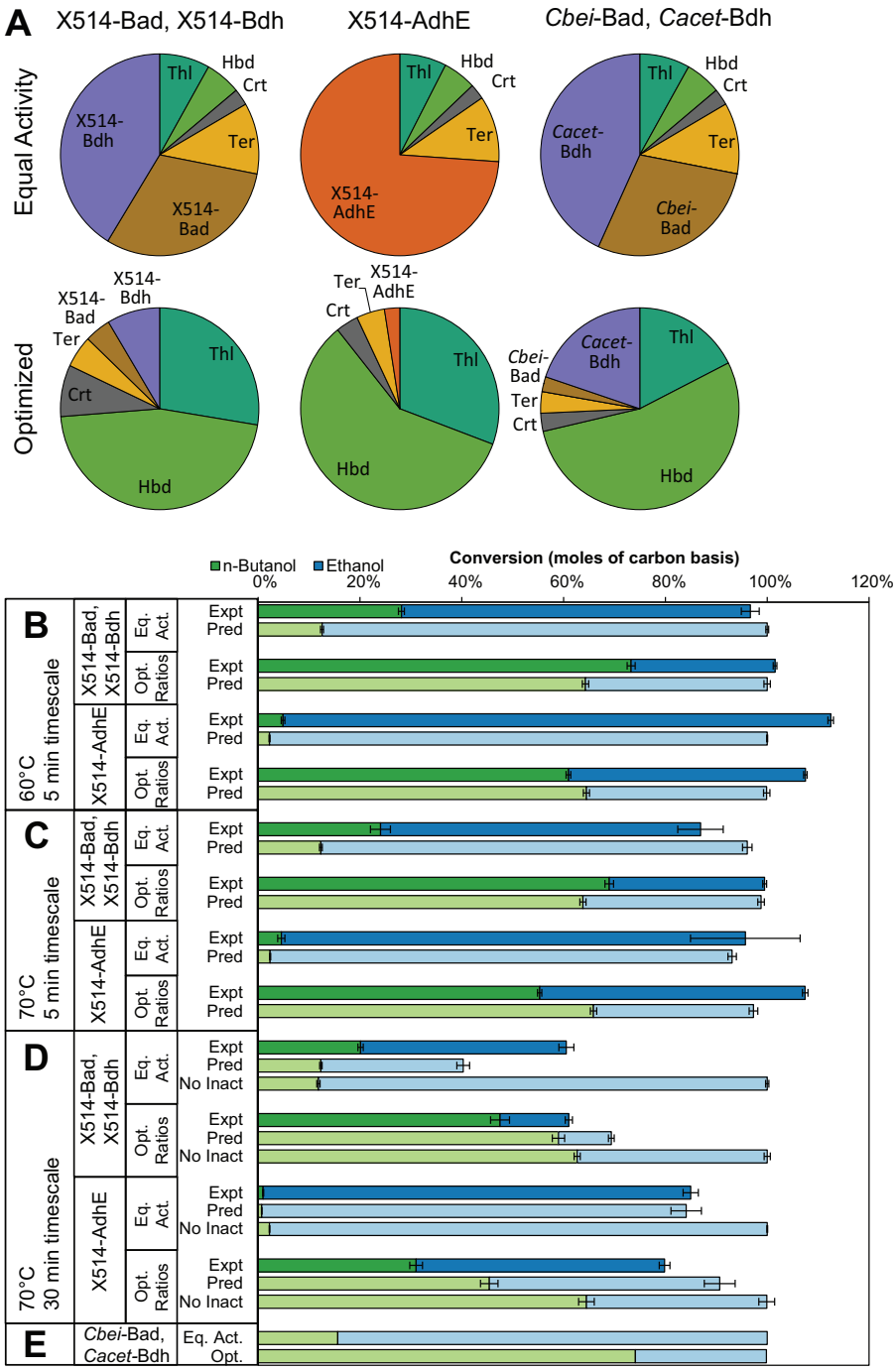

FIG 4 Measured and predicted alcohol production for *in vitro* assembly of pathway enzymes. (A) Molar enzyme proportions of each pathway variant for equal activities of each enzyme and optimized ratios for maximum *n*-butanol selectivity. (B) Measured (experimental [Expt]) and model-predicted (Pred) production of alcohols *in vitro* at 60°C using high enzyme loading for predicted reaction completion in 5 min. (C) Production at 70°C using high enzyme loads. (D) Production at 70°C using low enzyme loads for predicted reaction completion in 30 min, also compared with model predictions without accounting for enzyme inactivation (No Inact). (E) Model predictions of alcohol production using hypothetical thermostable versions of *C. beijerinckii* Bad (47) and *C. acetobutylicum* Bdh (44). Each error bar represents one standard error.

The results of the model-predicted enzyme ratio optima for each pathway variant (X514-Bad/X514-Bdh or X514-AdhE) are reported in Fig. 4A. In each case, the model predicts that using high relative concentrations of Thl and Hbd, along with a low relative concentration of Bad or AdhE, results in the highest selectivity for *n*-butanol. The optimum enzyme ratios were tested *in vitro*, using a total enzyme load such that *n*-butanol production is predicted to be complete in 5 min to minimize the effects of enzyme inactivation. The optimized Bad/Bdh pathway was able to convert 73% and 69% of acetyl-CoA to *n*-butanol at 60°C and

TABLE 5 Enzyme-catalyzed reaction rate expressions[a]

Bi Bi Ping Pong (Thl) 2 C_2-CoA = AcAc-CoA + CoA	$r = \frac{k_{cat}^{fwd} E\left(A^2 - \frac{PQ}{K_{eq}}\right)}{A^2 + K_A A\left(1 + \frac{P}{K_{IP}} + \frac{Q}{K_{IQ}}\right) + \frac{k_{cat}^{fwd}}{k_{cat}^{rev} K_{eq}}\left[PQ + K_P Q + K_Q P\right]}$	A = C_2-CoA P = AcAc-CoA Q = CoA
Irreversible Bi (Hbd, Ter, Bdh/AdhE) Hbd: AcAc-CoA + NADH = 3HB-CoA + NAD Ter: Crot-CoA + NADH = C_4-CoA + NAD Bdh/AdhE: Acetal + NADH = EtOH + NAD Butyral + NADH = ButOH + NAD	$r = \frac{k_{cat}^{fwd} E A_1 B}{A_1 B + K_{A1}\left(1 + \frac{A_2}{K_{A2}}\right) B + K_B A_1}$	**Hbd:** A_1 = AcAc-CoA B = NADH (no A_2) **Ter:** A_1 = Crot-CoA B = NADH (no A_2) **Bdh/AdhE Acetal reduction:** A_1 = Acetal A_2 = Butyral B = NADH A_1 and A_2 switched for Butyral reduction.
Uni Uni (Crt) 3HB-CoA = Crot-CoA + H_2O	$r = \frac{k_{cat}^{fwd} E\left(A - \frac{P}{K_{eq}}\right)}{K_A + A + \frac{K_A}{K_P} P}$	A = 3HB-CoA P = Crot-CoA
Ordered Bi Ter (Bad/AdhE) C_2-CoA + NADH = Acetal + NAD + CoA C_4-CoA + NADH = Butyral + NAD + CoA	$r = \frac{k_{cat}^{fwd} E\left(AB_1 - \frac{PQR_1}{K_{eq}}\right)}{AB_1 + K_A B_1 + K_{B1}\left(1 + \frac{B_2}{K_{B2}}\right) A + \frac{k_{cat}^{fwd}}{k_{cat}^{rev} K_{eq}}\left[PQR_1 + K_P Q R_1 + K_Q P R_1 + K_{R1}\left(1 + \frac{R_2}{K_{R2}}\right) PQ\right]}$	**C_2-CoA reduction:** A = NADH B_1 = C_2-CoA B_2 = C_4-CoA P = NAD Q = CoA R_1 = Acetal, R_2 = Butyral B_1/B_2 and R_1/R_2 switched for C_4-CoA reduction.

[a] Rate expressions were adapted from reference 73. For all equations, except bi bi ping pong, terms involving inhibition constants were eliminated from rate expression. When possible, the $k_{cat}^{fwd}/(K_{eq}\, k_{cat}^{rev})$ term (where fwd is forward, rev is reverse, and K_{eq} is the equilibrium constant) was eliminated from the denominator using a Haldane equality. k_{cat}^{fwd} and k_{cat}^{rev} (second^{-1}) are turnover numbers. *A*,*B*. . .*E* (moles/liter) are the substrate, product, and enzyme concentrations. K_A, K_B. . . (moles/liter) are Michealis constants. K_{IP} and K_{IQ} (moles/liter) are inhibition constants. The equilibrium constant at standard conditions is K_{eq} (moles/liter)^n, where n is the sum of stoichiometric coefficients for the reaction.

70°C, respectively, corresponding to selectivities of 2.6 and 2.3 (Fig. 4B and C and Table 7), a nearly 3-fold improvement in butanol production over the equal activity case. Likewise, the optimized X514-AdhE pathway was able to achieve 61% and 55% conversion to *n*-butanol at 60°C and 70°C, corresponding to selectivities of 1.3 and 1.1, a 12-fold improvement in *n*-butanol production. The Bad/Bdh pathway with optimized ratios was able to produce more *n*-butanol than the X514-AdhE pathway, likely because of the higher specificity of X514-Bad for butyryl-CoA than X514-AdhE. Model results for both pathways using the optimized and nonoptimized (equal activity) conditions are in good agreement with experimentally determined *n*-butanol and ethanol concentrations (Fig. 4B and C).

A drawback to using the low concentrations of Bad or AdhE required for high selectivity in the optimized cases is a decrease in the overall specific productivity of the pathway, defined as the average rate to produce 90% of the final alcohol concentration per gram of enzyme. For both the Bad/Bdh and X514-AdhE pathways, the overall alcohol productivity is lower for the optimized enzyme ratios than when using equal activity, illustrating a trade-off between pathway selectivity and pathway flux.

To show the effects of enzyme inactivation on the system, *in vitro* *n*-butanol production was carried out at 70°C with a lower enzyme load, adjusted so that *n*-butanol production is predicted to be complete in 30 min (Fig. 4D). As expected, under these conditions, both pathways failed to convert all of the acetyl-CoA to alcohols as a result of inactivation of Bad, Bdh, or X514-AdhE. The kinetic model also predicts incomplete conversion, although the agreement with experimental data is not as good as for the 5-min time scale reactions, possibly as a result of uncertainties in the measurement of enzyme inactivation parameters. If enzyme inactivation is not included in the model, complete conversion is predicted, primarily in the form of ethanol production. Interestingly, in the case of the Bad/Bdh pathway, *n*-butanol production is much higher relative to ethanol production than would be the case if all the enzymes were stable, leading to a higher selectivity for *n*-butanol. This example illustrates how the interplay between enzyme ratios and enzyme stability can increase the selectivity of the pathway, albeit at the cost of conversion efficiency.

To examine the time course predictive capability of the model, reactions with the optimized Bad/Bdh pathway were carried out at 60°C and sampled over time, with enzyme loads adjusted so that *n*-butanol production is predicted to be completed in 75 min. The resulting time course profiles of alcohol production compare well with the model (Fig. 5). *n*-Butanol production is complete after about 1.5 h, consistent with model predictions, with ethanol production completing in about 3 h. The model predicts the final ethanol concentration extremely well, although it does somewhat overpredict the final *n*-butanol concentration.

Model predictions using hypothetical Bad and Bdh. While optimizing enzyme ratios for the X514-Bad/X514-Bdh and X514-AdhE pathways allowed >70% of the carbon in acetyl-CoA to be directed to butanol, it came at the cost of pathway productivity. We took advantage of our kinetic model to examine the effects of using hypothetical Bad and Bdh enzymes with increased specificity to C_4 substrates on pathway selectivity by adjusting kinetic

TABLE 6 Enzyme kinetic parameters used in model[a]

Enzyme	Rate law	k_{cat}^{fwd} (s^{-1})	k_{cat}^{rev} (s^{-1})	K_m[b] Substrate	K_m[b] Concn(μM)	K_I (μM)	K_{eq}[c]	Reference(s)
Thl	Bi bi ping pong	53.9	987[d]	C_2-CoA	271		2.8×10^{-5}	This work; 74
				AcAc-CoA	33	133		
				CoA	15	73		
Hbd	Irreversible bi	35		AcAc-CoA	18.7		(*180*)	This work
Crt	Uni uni	267	267[e]	3HB-CoA	107		0.22	This work
				Crot-CoA	30			75
Ter	Irreversible bi	47.7		Crot-CoA	49.9		(*1.2×10^9*)	This work
				NADH	38.9			
X514-Bad	Ordered bi ter	4.54 (C_2-CoA)	116 (C_2)[f]	C_2-CoA	83.6		0.14 M	This work
				C_4-CoA	27.2			
		22.7 (C_4-CoA)	573 (C_4)[f]	C_2	3,700		6.0 M	47
				C_4	3,700			
X514-Bdh	Irreversible bi	7.7 (C_2)		C_2	3,330		(*790*)	This work
		10.4 (C_4)		C_4	2,030		(*2,200*)	
Ctherm-AdhE	Ordered bi ter	3.3 (C_2-CoA)	82.2 (C_2)[f]	C_2-CoA	11.5		0.14 M	This work
		2.3 (C_4-CoA)	57.8 (C_4)[f]	C_4-CoA	15.0		6.0 M	47
	Irreversible bi	3.6 (C_2)		C_2	7,760		(*790*)	This work
		15.4 (C_4)		C_4	6,920		(*2,200*)	
X514-AdhE	Ordered bi ter	3.6 (C_2-CoA)	90.3 (C_2)[f]	C_2-CoA	9.4		0.14 M	This work
		2.3 (C_4-CoA)	56.8 (C_4)[f]	C_4-CoA	5.71		6.0 M	47
	Irreversible bi	23.0 (C_2)		C_2	22,000		(*790*)	This work
		22.9 (C_4)		C_4	3,230		(*2,200*)	

[a] Abbreviations: C_2-CoA, acetyl-CoA; AcAc-CoA, acetoacetyl-CoA; 3HB-CoA, 3-hydroxybutyryl-CoA; Crot-CoA, crotonyl-CoA; C_2-CoA, butyryl-CoA; C_2, acetaldehyde; C_4, butyraldehyde; CoA, coenzyme A.
[b] K_m values for NADH, NAD, and CoA are assumed to be 50 μM unless otherwise specified.
[c] Equilibrium constants calculated using eQuilibrator (76) at pH 7.9 and ionic strength of 0.1 M. The italic values shown in parentheses do not affect the reaction rate, because the reaction is modeled as irreversible.
[d] Based on reference 74, assuming a constant ratio of k_{cat}^{fwd} to k_{cat}^{rev}.
[e] Assumed to be equal to k_{cat}^{fwd}.
[f] Based on reference 47, assuming a constant ratio of k_{cat}^{fwd} to k_{cat}^{rev}.

parameters *in silico*. The Bad and Bdh enzyme kinetic parameters were adjusted to match the substrate specificities of the mesophilic enzymes *C. beijerinckii* Bad (*Cbei*-Bad) (47) and *C. acetobutylicum* Bdh (*Cacet*-Bdh) (44), which are known to be more specific for C_4 substrates. The kinetic model was used to predict selectivity of a pathway composed of these hypothetical thermostable and C_4-specific enzymes for cases using equal activity of each enzyme and for model-predicted optimum enzyme ratios (Fig. 4A and E). The equal activity case using these hypothetical enzymes resulted in 16% conversion to *n*-butanol, corresponding to a low selectivity

TABLE 7 Pathway selectivity and productivity[a]

Pathway variant	Enzyme ratios	Selectivity (*n*-butanol/ethanol ratio)[b] Measured	Selectivity (*n*-butanol/ethanol ratio)[b] Predicted	Specific productivity (mol of C/h/g of enzyme) (predicted)[c] *n*-Butanol	Ethanol	Overall
X514-Bad/X514-Bdh	Equal activity	0.41 ± 0.02	0.14 ± 0.06	35	95	112
	Optimized	2.59 ± 0.02	1.80 ± 0.11	53	12	45
X514-AdhE	Equal activity	0.05 ± 0.01	0.02 ± 0.01	9.4	99	102
	Optimized	1.31 ± 0.01	1.82 ± 0.06	21	2.8	13
Cbei-Bad/*Cacet*-Bdh	Equal activity		0.19	12	2.1	2.7
	Optimized		2.88	29	0.4	3.2

[a] For reactions run at 60°C, 5-min reaction time scale.
[b] Moles of carbon in the *n*-butanol/ethanol ratio.
[c] Average rate to produce 90% of the final alcohol concentration.

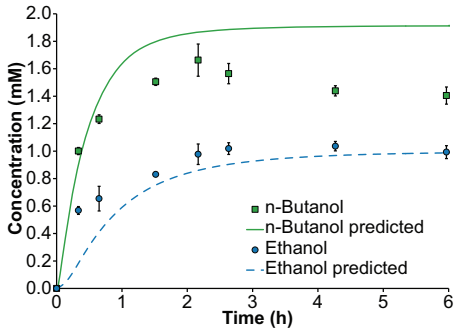

FIG 5 *In vitro* production of ethanol and *n*-butanol using X514-Bad/X514-Bdh pathway with optimized enzyme ratios at 60°C and low enzyme loads (predicted *n*-butanol production complete in 75 min). Each error bar represents one standard error.

of 0.2. When optimized enzyme ratios are applied, conversion to *n*-butanol and selectivity increase to 74% and 2.9, respectively, slightly higher than measured for the X514-Bad/X514-Bdh pathway. Importantly, however, the increase in selectivity for the *Cbei*-Bad/*Cacet*-Bdh pathway did not come at the cost of pathway productivity; instead, a slight increase in productivity is accomplished (Table 7). This illustrates the need for thermophilic versions of these enzymes with higher specificities for C_4 substrates to allow efficient *n*-butanol production.

DISCUSSION

We show herein the successful *in vitro* assembly of a hybrid enzymatic pathway for *n*-butanol production based on the synthetic pathway recently established in the thermophile *P. furiosus* (35). Two variants of the pathway, one using Bad and Bdh from *Thermoanaerobacter* sp. strain X514, and another using AdhE from the same organism, could produce *n*-butanol from acetyl-CoA and NADH. While we did not examine the *Ctherm*-AdhE pathway variant for butanol production because of the enzyme's poor thermal stability, *Ctherm*-AdhE has been used for engineered production of ethanol in *Caldicellulosiruptor bescii* (11). However, no ethanol production was observed at growth temperatures above 65°C, an unsurprising result in light of the extreme thermal lability of the enzyme at 70°C reported here.

Each pathway also produced ethanol as an undesired side product because the Bad, Bdh, and AdhE enzymes are not specific for their C_4 substrates. The approach using equal activity of each enzyme in the reaction resulted in low selectivities for *n*-butanol production ranging from 0.05 to 0.41, with ethanol as the major reaction product, accounting for 72 to 95% of the total carbon. The selectivity of both pathways could be increased *in vitro* by using high relative concentrations of Thl (28 mol%) and Hbd (46 mol%) and low concentrations of X514-AdhE (2.5 mol%) or X514-Bad (4.2 mol%) and X514-Bdh (8.6 mol%). This strategy could be applied *in vivo* by adjusting enzyme expression levels via promoter strength, ribosomal binding sequences, and gene copy number. Adjusting enzyme expression levels has been used to improve production of a variety of target molecules (55–57). Expression of the Bad/Bdh pathway in the extreme thermophile *P. furiosus* resulted in roughly equal activities of each enzyme, as measured in cell extracts at 60°C (35). Using the measured activities in cell extracts, our kinetic model predicts a butanol selectivity of 0.22, close to the observed *in vivo* *n*-butanol selectivity of ~0.11. As methods for changing heterologous enzyme expression in *P. furiosus* become available, this strategy can be applied *in vivo* to increase *n*-butanol selectivity. However, the increase in selectivity comes at the cost of pathway flux, a classical trade-off in reaction engineering problems.

Clearly, one strategy for increasing the pathway selectivity for *n*-butanol production without sacrificing flux is to use Bad and Bdh enzymes with increased specificity for C_4 substrates. The Bad enzyme from *C. beijerinckii* and the Bdh enzyme from *C. acetobutylicum*, two mesophilic organisms that natively produce high *n*-butanol titers, are known to be more specific for C_4 substrates than the thermophilic enzymes examined here (44, 47). Using optimized enzyme ratios, the *Cbei*-Bad/*Cacet*-Bdh pathway allows the highest selectivity for *n*-butanol production with an increased pathway flux (Table 7). However, even though *Cbei*-Bad and *Cacet*-Bdh are more selective, optimized ratios of the enzymes are still required to achieve a high selectivity. Given the advantages of using thermophilic hosts for easier downstream separations such as gas stripping, it would be useful to develop a more selective pathway for *n*-butanol production. Thermophilic Bad and Bdh enzymes with increased specificity for C_4 substrates could be developed with protein engineering strategies or searched for by screening additional candidates in available genomes or even metagenomic sequences.

Another way to increase *n*-butanol selectivity, at least *in vitro*, is the use of less stable enzymes, Bad and Bdh, for the aldehyde and alcohol dehydrogenase steps. When the Bad/Bdh pathway was used with optimized ratios at 70°C but with lower enzyme concentrations, a high selectivity was obtained (Fig. 4D). This strategy takes advantage of transient behavior of the pathway: most of the acetyl-CoA is pulled into the four-carbon branch of the pathway early on in the reaction, as a result of the high proportions of Thl and Hbd used. The resulting high concentration of butyryl-CoA relative to acetyl-CoA, combined with the slight substrate specificity of Bad, causes most of the *n*-butanol to be produced quickly, with ethanol production increasing only as butyryl-CoA becomes depleted (also seen in Fig. 5). As a result, most of the *n*-butanol is produced before any significant inactivation of Bad or Bdh occurs. As the reaction proceeds, the Bad and Bdh enzymes are inactivated and ethanol production slows to a halt, resulting in a much higher *n*-butanol/ethanol ratio than would occur if the Bad and Bdh enzymes were stable. Whether this strategy could be used to increase *n*-butanol selectivity *in vivo*, where metabolite concentrations exist in pseudo-steady-state, remains to be seen.

The ability of the kinetic model developed here to interrogate aspects of the hybrid butanol pathway illustrates the power of modeling approaches to provide insight into candidate pathways for metabolic engineering projects. In this case, the model allowed limitations of the pathway to become apparent, and it suggests ways to overcome the limitations, e.g., by adjusting enzyme ratios to improve selectivity. Kinetic models have been developed for a variety of enzymatic pathways, such as glycolysis, sphingolipid and ergosterol metabolism, and pentose phosphate pathway in the yeast *Saccharomyces cerevisiae* (53), acetone-butanol-ethanol fermentation in clostridia (54, 58), and the Calvin cycle in plants (59). Unlike the *n*-butanol pathway model introduced here, which used *a priori*-determined enzyme kinetic parameters, most of these kinetic models require parameter fitting to experimental data of the operating pathway or organism (53). For example, the

model of ABE fermentation pathways by *C. acetobutylicum* was fit to experimental data of batch cultures on various sugars (54).

There are several reasons why kinetic models are often fit to experimental data rather than using *a priori*-determined enzyme kinetic parameters. The major reason is illustrated by a notable exception to the use of parameter fitting for kinetic modeling: the modeling of monolignol synthesis in *Populus trichocarpa*, in which Michaelis-Menten kinetic and inhibition parameters were determined for 21 purified enzymes (60). The difficulty and effort required to purify and characterize each enzyme to be modeled is a major undertaking. While not all enzymes have a large effect on the overall pathway flux, identifying the crucial enzymes using techniques, such as metabolic control analysis, still requires knowledge of enzyme kinetic properties (61). An additional obstacle to the development of kinetic modeling can be the difficulty in characterizing enzymes under *in vivo*-like conditions (62).

Recent calls have been made for more integration of top-down genome-scale metabolic models, which can be used for constraint-based, system-wide analysis, with the bottom-up approach of enzyme kinetic models, which are more descriptive and can model a wider variety of conditions (53, 62, 63). Steps have been taken toward developing integrated genome-scale kinetic models, such as for *E. coli* (64), yeast (65), and *Mycoplasma genitalium* (66). These models still rely on parameter fitting to estimate many enzyme parameters. However, the existence of a large-scale metabolic kinetic model of an organism would be pivotal for identifying successful strategies for metabolic engineering.

ACKNOWLEDGMENTS

This work was supported by grants to R.M.K. and M.W.W.A. by the U.S. Department of Energy Research ARPA-E Electrofuels Program (DE-AR0000081) and the U.S. National Science Foundation (CBET-1264052 and CBET-1264053). A.J.L. and B.M.Z. acknowledge support from an NIH Biotechnology Traineeship (2T32GM008776).

REFERENCES

1. **Bhandiwad A, Shaw AJ, Guss A, Guseva A, Bahl H, Lynd LR.** 2014. Metabolic engineering of *Thermoanaerobacterium saccharolyticum* for *n*-butanol production. Metab Eng **21:**17–25. http://dx.doi.org/10.1016/j.ymben.2013.10.012.
2. **Lin PP, Rabe KS, Takasumi JL, Kadisch M, Arnold FH, Liao JC.** 2014. Isobutanol production at elevated temperatures in thermophilic *Geobacillus thermoglucosidasius*. Metab Eng **24:**1–8. http://dx.doi.org/10.1016/j.ymben.2014.03.006.
3. **Deng Y, Olson DG, Zhou JL, Herring CD, Shaw AJ, Lynd LR.** 2013. Redirecting carbon flux through exogenous pyruvate kinase to achieve high ethanol yields in *Clostridium thermocellum*. Metab Eng **15:**151–158. http://dx.doi.org/10.1016/j.ymben.2012.11.006.
4. **Thorgersen MP, Lipscomb GL, Schut GJ, Kelly RM, Adams MWW.** 2014. Deletion of acetyl-CoA synthetases I and II increases production of 3-hydroxypropionate by the metabolically-engineered hyperthermophile *Pyrococcus furiosus*. Metab Eng **22:**83–88. http://dx.doi.org/10.1016/j.ymben.2013.12.006.
5. **Ludlow JM, Clark DS.** 1991. Engineering considerations for the application of extremophiles in biotechnology. Crit Rev Biotechnol **10:**321–345. http://dx.doi.org/10.3109/07388559109038214.
6. **Abdel-Banat BM, Hoshida H, Ano A, Nonklang S, Akada R.** 2010. High-temperature fermentation: how can processes for ethanol production at high temperatures become superior to the traditional process using mesophilic yeast? Appl Microbiol Biotechnol **85:**861–867. http://dx.doi.org/10.1007/s00253-009-2248-5.
7. **Hawkins AS, Han Y, Lian H, Loder AJ, Menon AL, Iwuchukwu IJ, Keller M, Leuko TT, Adams MWW, Kelly RM.** 2011. Extremely thermophilic routes to microbial electrofuels. ACS Catal **1:**1043–1050. http://dx.doi.org/10.1021/cs2003017.
8. **Basen M, Sun J, Adams MWW.** 2012. Engineering a hyperthermophilic archaeon for temperature-dependent product formation. mBio **3**(2): e00053-12. http://dx.doi.org/10.1128/mBio.00053-12.
9. **Keller MW, Schut GJ, Lipscomb GL, Menon AL, Iwuchukwu IJ, Leuko TT, Thorgersen MP, Nixon WJ, Hawkins AS, Kelly RM, Adams MWW.** 2013. Exploiting microbial hyperthermophilicity to produce an industrial chemical, using hydrogen and carbon dioxide. Proc Natl Acad Sci U S A **110:**5840–5845. http://dx.doi.org/10.1073/pnas.1222607110.
10. **Hawkins AB, Lian H, Zeldes BM, Loder AJ, Lipscomb GL, Schut GJ, Keller MW, Adams MWW, Kelly RM.** 2015. Bioprocessing analysis of *Pyrococcus furiosus* strains engineered for CO_2-based 3-hydroxypropionate production. Biotechnol Bioeng **112:**1533–1543. http://dx.doi.org/10.1002/bit.25584.
11. **Chung D, Cha M, Guss AM, Westpheling J.** 2014. Direct conversion of plant biomass to ethanol by engineered *Caldicellulosiruptor bescii*. Proc Natl Acad Sci U S A **111:**8931–8936. http://dx.doi.org/10.1073/pnas.1402210111.
12. **Solomon KV, Prather KLJ.** 2011. The zero-sum game of pathway optimization: emerging paradigms for tuning gene expression. Biotechnol J **6:**1064–1070. http://dx.doi.org/10.1002/biot.201100086.
13. **Liu Y, Zhu Y, Li J, Shin H-D, Chen RR, Du G, Liu L, Chen J.** 2014. Modular pathway engineering of *Bacillus subtilis* for improved *N*-acetylglucosamine production. Metab Eng **23:**42–52. http://dx.doi.org/10.1016/j.ymben.2014.02.005.
14. **Lee JW, Na D, Park JM, Lee J, Choi S, Lee SY.** 2012. Systems metabolic engineering of microorganisms for natural and non-natural chemicals. Nat Chem Biol **8:**536–546. http://dx.doi.org/10.1038/nchembio.970.
15. **Biggs BW, De Paepe B, Santos CNS, De Mey M, Kumaran AP.** 2014. Multivariate modular metabolic engineering for pathway and strain optimization. Curr Opin Biotechnol **29:**156–162. http://dx.doi.org/10.1016/j.copbio.2014.05.005.
16. **Buelter T, Meinhold P, Feldman RMR, Eckl E, Hawkins A, Aristidou A, Dundon CA, Lies D, Bastian S, Arnold F.** 2010. Engineered microorganisms capable of producing target compounds under anaerobic conditions. US patent application 20100143997.
17. **Feldman RMR, Gunawardena U, Urano J, Meinhold P, Aristidou AA, Dundon CA, Smith C.** September 2011. Yeast organism producing isobutanol at a high yield. US patent 8,017,375.
18. **Liao DI, Nelson MJ, Bramucci MG.** March 2011. Fermentive production of isobutanol using highly active ketol-acid reductoisomerase enzymes. US patent 7,910,342.
19. **Lee SY, Park JH, Jang SH, Nielsen LK, Kim J, Jung KS.** 2008. Fermentative butanol production by clostridia. Biotechnol Bioeng **101:**209–228. http://dx.doi.org/10.1002/bit.22003.
20. **Mainguet SE, Liao JC.** 2010. Bioengineering of microorganisms for C_3 to C_5 alcohols production. Biotechnol J **5:**1297–1308. http://dx.doi.org/10.1002/biot.201000276.
21. **Peralta-Yahya PP, Keasling JD.** 2010. Advanced biofuel production in microbes. Biotechnol J **5:**147–162. http://dx.doi.org/10.1002/biot.200900220.
22. **Vane LM.** 2008. Separation technologies for the recovery and dehydration of alcohols from fermentation broths. Biofuel Bioprod Biorefining **2:**553–588. http://dx.doi.org/10.1002/bbb.108.
23. **Li F, Hinderberger J, Seedorf H, Zhang J, Buckel W, Thauer RK.** 2008. Coupled ferredoxin and crotonyl coenzyme A (CoA) reduction with NADH catalyzed by the butyryl-CoA dehydrogenase/Etf complex from *Clostridium kluyveri*. J Bacteriol **190:**843–850. http://dx.doi.org/10.1128/JB.01417-07.
24. **Shen CR, Lan EI, Dekishima Y, Baez A, Cho KM, Liao JC.** 2011. Driving forces enable high-titer anaerobic 1-butanol synthesis in *Escherichia coli*. Appl Environ Microbiol **77:**2905–2915. http://dx.doi.org/10.1128/AEM.03034-10.
25. **Jang YS, Kim B, Shin JH, Choi YJ, Choi S, Song CW, Lee J, Park HG, Lee SY.** 2012. Bio-based production of C2-C6 platform chemicals. Biotechnol Bioeng **109:**2437–2459. http://dx.doi.org/10.1002/bit.24599.
26. **Tomas CA, Welker NE, Papoutsakis ET.** 2003. Overexpression of *groESL* in *Clostridium acetobutylicum* results in increased solvent production and tolerance, prolonged metabolism, and changes in the cell's transcriptional program. Appl Environ Microbiol **69:**4951–4965. http://dx.doi.org/10.1128/AEM.69.8.4951-4965.2003.
27. **Jang YS, Lee JY, Lee J, Park JH, Im JA, Eom MH, Lee J, Lee SH, Song H, Cho JH, Seung DY, Lee SY.** 2012. Enhanced butanol production obtained by reinforcing the direct butanol-forming route in *Clostridium acetobutylicum*. mBio **3**(5):e00314-12. http://dx.doi.org/10.1128/mBio.00314-12.

28. **Bond-Watts BB, Bellerose RJ, Chang MCY.** 2011. Enzyme mechanism as a kinetic control element for designing synthetic biofuel pathways. Nat Chem Biol **7:**222–227. http://dx.doi.org/10.1038/nchembio.537.
29. **Bond-Watts BB, Weeks AM, Chang MCY.** 2012. Biochemical and structural characterization of the *trans*-enoyl-CoA reductase from *Treponema denticola*. Biochemistry **51:**6827–6837. http://dx.doi.org/10.1021/bi300879n.
30. **Dürre P, Fischer RJ, Kuhn A, Lorenz K, Schreiber W, Stürzenhofecker B, Ullmann S, Winzer K, Sauer U.** 1995. Solventogenic enzymes of *Clostridium acetobutylicum*: catalytic properties, genetic organization, and transcriptional regulation. FEMS Microbiol Rev **17:**251–262. http://dx.doi.org/10.1111/j.1574-6976.1995.tb00209.x.
31. **Dürre P, Kuhn A, Gottwald M, Gottschalk G.** 1987. Enzymatic investigations on butanol dehydrogenase and butyraldehyde dehydrogenase in extracts of *Clostridium acetobutylicum*. Appl Microbiol Biotechnol **26:**268–272. http://dx.doi.org/10.1007/BF00286322.
32. **Trinh CT.** 2012. Elucidating and reprogramming *Escherichia coli* metabolisms for obligate anaerobic *n*-butanol and isobutanol production. Appl Microbiol Biotechnol **95:**1083–1094. http://dx.doi.org/10.1007/s00253-012-4197-7.
33. **Freier-Schröder D, Wiegel J, Gottschalk G.** 1989. Butanol formation by *Clostridium thermosaccharolyticum* at neutral pH. Biotechnol Lett **11:**831–836. http://dx.doi.org/10.1007/BF01026107.
34. **Pley U, Schipka J, Gambacorta A, Jannasch HW, Fricke H, Rachel R, Stetter KO.** 1991. *Pyrodictium abyssi* sp. nov. represents a novel heterotrophic marine archaeal hyperthermophile growing at 110°C. Syst Appl Microbiol **14:**245–253. http://dx.doi.org/10.1016/S0723-2020(11)80376-0.
35. **Keller MW, Lipscomb GL, Loder AJ, Schut GJ, Kelly RM, Adams MWW.** 2015. A hybrid synthetic pathway for butanol production by a hyperthermophilic microbe. Metab Eng **27:**101–106. http://dx.doi.org/10.1016/j.ymben.2014.11.004.
36. **Gibson DG.** 2011. Enzymatic assembly of overlapping DNA fragments. Methods Enzymol **498:**349–361. http://dx.doi.org/10.1016/B978-0-12-385120-8.00015-2.
37. **Studier FW.** 2005. Protein production by auto-induction in high-density shaking cultures. Protein Expr Purif **41:**207–234. http://dx.doi.org/10.1016/j.pep.2005.01.016.
38. **Ziegenhorn J, Senn M, Bücher T.** 1976. Molar absorptivities of β-NADH and β-NADPH. Clin Chem **22:**151–160.
39. **Baty F, Ritz C, Charles S, Brutsche M, Flandrois JP, Delignette-Muller M-L.** 2015. A toolbox for nonlinear regression in R: the package nlstools. J Stat Softw **66:**1–21.
40. **Epting KL, Vieille C, Zeikus JG, Kelly RM.** 2005. Influence of divalent cations on the structural thermostability and thermal inactivation kinetics of class II xylose isomerases. FEBS J **272:**1454–1464. http://dx.doi.org/10.1111/j.1742-4658.2005.04577.x.
41. **Bradford MM.** 1976. A rapid and sensitive method for the quantitation of microgram quantities of protein utilizing the principle of protein-dye binding. Anal Biochem **72:**248–254. http://dx.doi.org/10.1016/0003-2697(76)90527-3.
42. **Lo J, Zheng T, Hon S, Olson DG, Lynd LR, Metcalf WW.** 2015. The bifunctional alcohol and aldehyde dehydrogenase gene, *adhE*, is necessary for ethanol production in *Clostridium thermocellum* and *Thermoanaerobacterium saccharolyticum*. J Bacteriol **197:**1386–1393. http://dx.doi.org/10.1128/JB.02450-14.
43. **Brown SD, Guss AM, Karpinets TV, Parks JM, Smolin N, Yang S, Land ML, Klingeman DM, Bhandiwad A, Rodriguez M, Raman B, Shao X, Mielenz JR, Smith JC, Keller M, Lynd LR.** 2011. Mutant alcohol dehydrogenase leads to improved ethanol tolerance in *Clostridium thermocellum*. Proc Natl Acad Sci U S A **108:**13752–13757. http://dx.doi.org/10.1073/pnas.1102444108.
44. **Welch RW, Rudolph FB, Papoutsakis ET.** 1989. Purification and characterization of the NADH-dependent butanol dehydrogenase from *Clostridium acetobutylicum* (ATCC 824). Arch Biochem Biophys **273:**309–318. http://dx.doi.org/10.1016/0003-9861(89)90489-X.
45. **Hiu SF, Zhu CX, Yan RT, Chen JS.** 1987. Butanol-ethanol dehydrogenase and butanol-ethanol-isopropanol dehydrogenase: different alcohol dehydrogenases in two strains of *Clostridium beijerinckii* (*Clostridium butylicum*). Appl Environ Microbiol **53:**697–703.
46. **Hartmanis MGN, Kason T, Gatenbeck S.** 1984. Uptake and activation of acetate and butyrate in *Clostridium acetobutylicum*. Appl Microbiol Biotechnol **20:**66–71.
47. **Yan RT, Chen JS.** 1990. Coenzyme A-acylating aldehyde dehydrogenase from *Clostridium beijerinckii* NRRL B592. Appl Environ Microbiol **56:**2591–2599.
48. **Peng H, Wu G, Shao W.** 2008. The aldehyde/alcohol dehydrogenase (AdhE) in relation to the ethanol formation in *Thermoanaerobacter ethanolicus* JW200. Anaerobe **14:**125–127. http://dx.doi.org/10.1016/j.anaerobe.2007.09.004.
49. **Fontaine L, Meynial-Salles I, Girbal L, Yang X, Croux C, Soucaille P.** 2002. Molecular characterization and transcriptional analysis of *adhE2*, the gene encoding the NADH-dependent aldehyde/alcohol dehydrogenase responsible for butanol production in alcohologenic cultures of *Clostridium acetobutylicum* ATCC 824. J Bacteriol **184:**821–830. http://dx.doi.org/10.1128/JB.184.3.821-830.2002.
50. **Kessler D, Leibrecht I, Knappe J.** 1991. Pyruvate-formate-lyase-deactivase and acetyl-CoA reductase activities of *Escherichia coli* reside on a polymeric protein particle encoded by *adhE*. FEBS Lett **281:**59–63. http://dx.doi.org/10.1016/0014-5793(91)80358-A.
51. **Extance J, Crennell SJ, Eley K, Cripps R, Hough DW, Danson MJ.** 2013. Structure of a bifunctional alcohol dehydrogenase involved in bioethanol generation in *Geobacillus thermoglucosidasius*. Acta Crystallogr D Biol Crystallogr **69:**2104–2115. http://dx.doi.org/10.1107/S0907444913020349.
52. **Bruchhaus I, Tannich E.** 1994. Purification and molecular characterization of the NAD^+-dependent acetaldehyde/alcohol dehydrogenase from *Entamoeba histolytica*. Biochem J **303:**743–748. http://dx.doi.org/10.1042/bj3030743.
53. **Kerkhoven EJ, Lahtvee P-J, Nielsen J.** 23 August 2014. Applications of computational modeling in metabolic engineering of yeast. FEMS Yeast Res http://dx.doi.org/10.1111/1567-1364.12199.
54. **Raganati F, Procentese A, Olivieri G, Götz P, Salatino P, Marzocchella A.** 2015. Kinetic study of butanol production from various sugars by *Clostridium acetobutylicum* using a dynamic model. Biochem Eng J **99:**156–166. http://dx.doi.org/10.1016/j.bej.2015.03.001.
55. **Alper H, Fischer C, Nevoigt E, Stephanopoulos G.** 2005. Tuning genetic control through promoter engineering. Proc Natl Acad Sci U S A **102:**12678–12683. http://dx.doi.org/10.1073/pnas.0504604102.
56. **Ajikumar PK, Xiao WH, Tyo KE, Wang Y, Simeon F, Leonard E, Mucha O, Phon TH, Pfeifer B, Stephanopoulos G.** 2010. Isoprenoid pathway optimization for Taxol precursor overproduction in *Escherichia coli*. Science **330:**70–74. http://dx.doi.org/10.1126/science.1191652.
57. **Lee SH, Kim M-S, Jung HC, Lee J, Lee J-H, Lee HS, Kang SG.** 2015. Screening of a novel strong promoter by RNA sequencing and its application to H_2 production in a hyperthermophilic archaeon. Appl Microbiol Biotechnol **99:**4085–4092. http://dx.doi.org/10.1007/s00253-015-6444-1.
58. **Mayank R, Ranjan A, Moholkar VS.** 2013. Mathematical models of ABE fermentation: review and analysis. Crit Rev Biotechnol **33:**419–447. http://dx.doi.org/10.3109/07388551.2012.726208.
59. **Schallau K, Junker BH.** 2010. Simulating plant metabolic pathways with enzyme-kinetic models. Plant Physiol **152:**1763–1771. http://dx.doi.org/10.1104/pp.109.149237.
60. **Wang JP, Naik PP, Chen HC, Shi R, Lin CY, Liu J, Shuford CM, Li Q, Sun YH, Tunlaya-Anukit S, Williams CM, Muddiman DC, Ducoste JJ, Sederoff RR, Chiang VL.** 2014. Complete proteomic-based enzyme reaction and inhibition kinetics reveal how monolignol biosynthetic enzyme families affect metabolic flux and lignin in *Populus trichocarpa*. Plant Cell **26:**894–914. http://dx.doi.org/10.1105/tpc.113.120881.
61. **Noor E, Bar-Even A, Flamholz A, Reznik E, Liebermeister W, Milo R.** 2014. Pathway thermodynamics highlights kinetic obstacles in central metabolism. PLoS Comput Biol **10:**e1003483. http://dx.doi.org/10.1371/journal.pcbi.1003483.
62. **Tummler K, Lubitz T, Schelker M, Klipp E.** 2014. New types of experimental data shape the use of enzyme kinetics for dynamic network modeling. FEBS J **281:**549–571. http://dx.doi.org/10.1111/febs.12525.
63. **Stitt M, Gibon Y.** 2014. Why measure enzyme activities in the era of systems biology? Trends Plant Sci **19:**256–265. http://dx.doi.org/10.1016/j.tplants.2013.11.003.
64. **Chakrabarti A, Miskovic L, Soh KC, Hatzimanikatis V.** 2013. Towards kinetic modeling of genome-scale metabolic networks without sacrificing stoichiometric, thermodynamic and physiological constraints. Biotechnol J **8:**1043–1057. http://dx.doi.org/10.1002/biot.201300091.
65. **Stanford NJ, Lubitz T, Smallbone K, Klipp E, Mendes P, Liebermeister W.** 2013. Systematic construction of kinetic models from genome-scale metabolic networks. PLoS One **8:**e79195. http://dx.doi.org/10.1371/journal.pone.0079195.
66. **Karr JR, Sanghvi JC, Macklin DN, Gutschow MV, Jacobs JM, Bolival B, Jr, Assad-Garcia N, Glass JI, Covert MW.** 2012. A whole-cell computa-

tional model predicts phenotype from genotype. Cell **150:**389–401. http://dx.doi.org/10.1016/j.cell.2012.05.044.
67. **Bhandiwad A, Guseva A, Lynd LR.** 2013. Metabolic engineering of *Thermoanaerobacterium thermosaccharolyticum* for increased *n*-butanol production. Adv Microbiol **3:**46–51. http://dx.doi.org/10.4236/aim.2013.31007.
68. **Berezina OV, Zakharova NV, Brandt A, Yarotsky SV, Schwarz WH, Zverlov VV.** 2010. Reconstructing the clostridial *n*-butanol metabolic pathway in *Lactobacillus brevis*. Appl Microbiol Biotechnol **87:**635–646. http://dx.doi.org/10.1007/s00253-010-2480-z.
69. **Si T, Luo Y, Xiao H, Zhao H.** 2014. Utilizing an endogenous pathway for 1-butanol production in *Saccharomyces cerevisiae*. Metab Eng **22:**60–68. http://dx.doi.org/10.1016/j.ymben.2014.01.002.
70. **Steen EJ, Chan R, Prasad N, Myers S, Petzold CJ, Redding A, Ouellet M, Keasling JD.** 2008. Metabolic engineering of *Saccharomyces cerevisiae* for the production of *n*-butanol. Microb Cell Fact **7:**36. http://dx.doi.org/10.1186/1475-2859-7-36.
71. **Nielsen DR, Leonard E, Yoon SH, Tseng HC, Yuan C, Prather KL.** 2009. Engineering alternative butanol production platforms in heterologous bacteria. Metab Eng **11:**262–273. http://dx.doi.org/10.1016/j.ymben.2009.05.003.
72. **Lan EI, Liao JC.** 2012. ATP drives direct photosynthetic production of 1-butanol in cyanobacteria. Proc Natl Acad Sci U S A **109:**6018–6023. http://dx.doi.org/10.1073/pnas.1200074109.
73. **Cook PF, Cleland WW.** 2007. Enzyme kinetics and mechanism. Taylor & Francis, New York, NY.
74. **Middleton B.** 1974. The kinetic mechanism and properties of the cytoplasmic acetoacetyl-coenzyme A thiolase from rat liver. Biochem J **139:**109–121. http://dx.doi.org/10.1042/bj1390109.
75. **Waterson RM, Castellino FJ, Hass GM, Hill RL.** 1972. Purification and characterization of crotonase from *Clostridium acetobutylicum*. J Biol Chem **247:**5266–5271.
76. **Flamholz A, Noor E, Bar-Even A, Milo R.** 2012. eQuilibrator—the biochemical thermodynamics calculator. Nucleic Acids Res **40:**D770–D775. http://dx.doi.org/10.1093/nar/gkr874.